Image Enhancement of Polyethersulfone Ultrafiltration Membrane Surface Structure for Atomic Force Microscopy

A. K. FRITZSCHE,*[1] A. R. AREVALO,[1] M. D. MOORE,[1] C. J. WEBER,[1]
V. B. ELINGS,[2] K. KJOLLER,[2] and C. M. WU[2]

[1]Cuno Separations Systems Division, 50 Kerry Place, Norwood, Massachusetts 02062 and [2]Digital Instruments, Inc., 6780 Cortona Drive, Santa Barbara, California 93117

SYNOPSIS

The surface topography and pore structure of ultrafiltration membranes can be investigated with atomic force microscopy. In this study, it was found that the substitution of ethanol for water as the immersion medium improved the resolution of the fine structure of 10K polyethersulfone ultrafiltration membranes. Pores in the membrane surface from 7 to 9 nm in diameter were measured, which coincides with the range expected for 10,000 molecular weight cutoff (MWCO) ultrafiltration membranes. It is believed that this image enhancement results from increased damping and concomitant noise reduction resulting from the higher viscosity of ethanol in contrast to water.

INTRODUCTION

The atomic force microscope yields topographic images by scanning a sample surface in contact with a sharp tip.[1,2] The images are obtained by the measurement of the deflection of the cantilever with a tip underneath as the features on the sample surface are moved under the tip. The force of the cantilever on the surface is kept both small and constant with a feedback mechanism that adjusts the height of the sample. As the tip is moved in a raster pattern, a trace of the surface sample is generated and a three-dimensional image is constructed. Unlike the scanning tunneling microscope (STM), atomic images can be produced on insulators as well as on conductors.[3,4]

Atomic force microscopy (AFM) also avoids the problems inherent in electron-beam instruments.[5] In contrast to the measurements utilizing force, electron beams are subject to chromatic aberrations that result from a dispersion of the energy of the electrons leaving the source. This energy spread results in decreased resolution. The higher beam energies needed to decrease the effects of chromatic aberration can damage sample surfaces under some conditions. In addition, bombarding a sample with electrons can lead to the charging of samples whose conductivity is low. When a conductive coating is applied to circumvent these potential problems, the finer detail in the sample may be obscured. Furthermore, both the coating of the sample and its subsequent examination are conducted under a high vacuum, which may alter the sample structure. In contrast, samples for AFM examination require neither coating nor high-vacuum exposure. Instead, the samples may be studied in the air. However, surfaces in air are typically covered with an adsorbed layer of water and unknown contaminants. When a tip covered with such a layer approaches a sample that is also so covered, there exists an adhesive force that drives the tip toward the sample.[6] The force of the tip upon the sample is given by the equation from Israelachvili[6]:

$$F = 4\pi R\delta \qquad (1)$$

where R is the radius of the tip, approximately $2.5 \times 10^{-8} M$, and δ is the surface tension of the immersing fluid. For example, immersion in water with a surface tension of 7.27×10^{-2} N/M at 20°C would yield a force of 2.3×10^{-8} N, which exceeds the maximum allowable interaction force of 10^{-8} N.[7]

* To whom correspondence should be addressed.

Journal of Applied Polymer Science, Vol. 46, 167–178 (1992)
 CCC 0021-8995/92/010167-12$04.00

The problems associated with this adhesive force can be avoided if the AFM is operated with the sample, tip, and cantilever immersed in a liquid. Water, seawater, ethanol, and paraffin oil have been used.[8,9] With this approach, AFM has successfully imaged surfaces with adsorbed organic molecules, such as sorbic acid, DNA, and proteins.[9] Also, the use of the smaller interaction forces by operation in water have permitted the observations of biological samples in physiologically relevant environments, such as the clotting of the human blood protein fibrogen.

This capability of AFM to image with low-interaction forces and in an aqueous environment suggested that it could be used to define the structure and morphology of ultrafiltration membranes.[10] The initial studies focused on polyethersulfone ultrafiltration membranes because such membranes with very narrow pore-size distributions are available in a range of molecular weight cutoffs (MWCO). Also, polyethersulfone ultrafiltration membranes must be maintained wet to prevent alteration in their pore structures, which occurs upon drying. Although the pore dimensions in 30K and 100K MWCO polyethersulfone ultrafiltration membranes were measured, the dimensions of the pores in the 10K MWCO ultrafiltration membrane remained elusive. The pores in this ultrafiltration membrane remained just below the limits of resolution of the AFM.

As seen in the schematic diagram given in Figure 1, laser light is focused on a cantilever and is reflected toward a photodiode. The photodiode detects the deflection of the cantilever by sensing the position of the reflected beam. In operation, a feedback loop keeps the position of the reflected beam and, hence, the force on the sample constant, which is accomplished by moving the sample up and down with the z-axis of the piezoelectric translator as the sample is scanned underneath it with the x- and y-axes. The optical lever amplifies the motion of the tip of the cantilever to produce the reflected beam

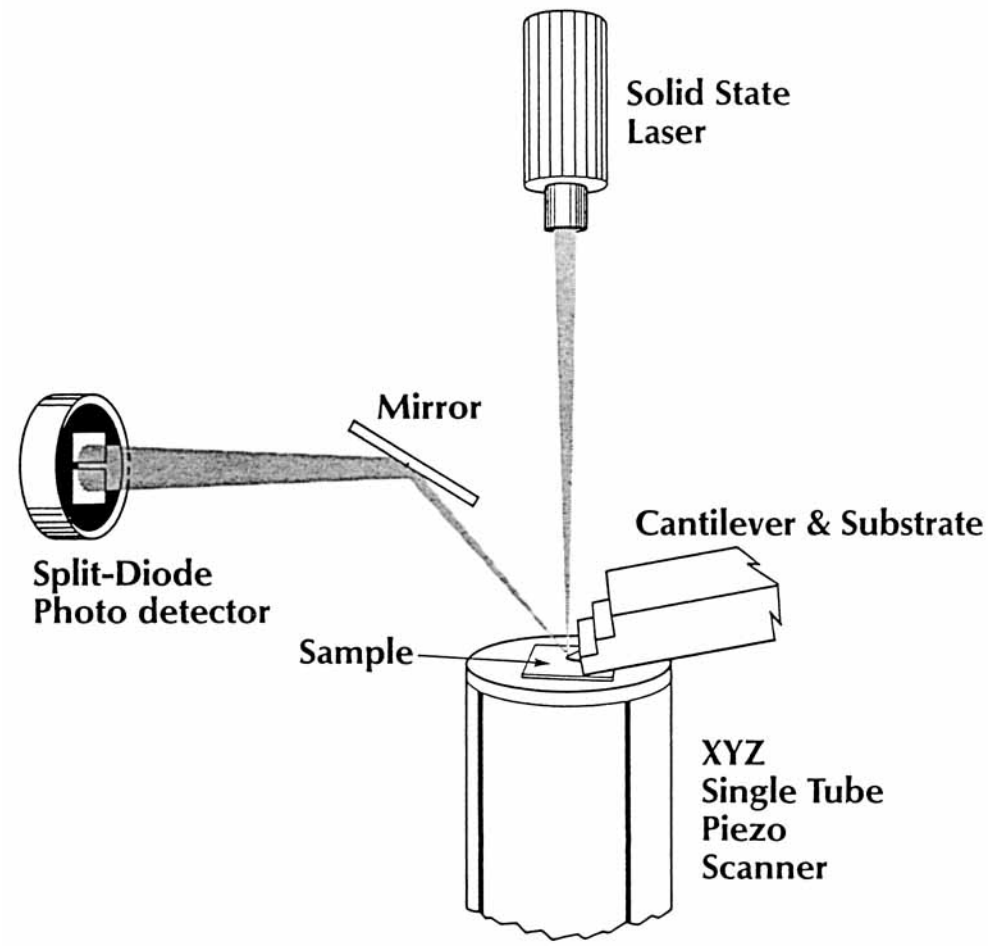

Figure 1 Schematic diagram of an AFM utilizing an optical lever technique for sensing cantilever deflection.

at the detector that is greater by a factor of $2L/l$, where $L \approx 4$ cm is the distance from the cantilever to the photodiode and l, which is approximately 100 μm, is the length of the cantilever.[9] This factor of 800 is sufficient so that sensitivity is not limited by the photodiode but by sound and building vibrations.[9]

Vibrational analysis may be used to gain an understanding of the motions in the AFM sensor, which can be represented by the model shown in Figure 2.[11] In this diagram, m is the mass of the cantilever and tip; x, its replacement, k, the spring constant; and C, the damping constant.
The general solution is

$$x = C_1 e^{[-(c/2m)+\sqrt{(c/2m)^2-(k/m)}]t} + C_2 e^{[-(c/2m)+\sqrt{(c/2m)^2-(k/m)}]t} \quad (2)$$

providing $c/2m \neq \sqrt{k/m}$.

The value of the damping constant that causes the radical part of the exponent in this equation to vanish is a convenient reference called the critical damping constant and is designated by c_c, which is defined by

$$\frac{c_c}{2m} = \sqrt{\frac{k}{m}} = \omega \quad (3)$$

For a damped system, the ratio of the damping constant to the critical value is a dimensionless parameter that represents a meaningful measure of the amount of damping present in the system; the ratio ζ is called the damping factor and is defined by

$$\zeta = \frac{c}{c_c} \quad (4)$$

The solution for eq. (2) for $0 < \zeta < 1$ is

$$x = \frac{e^{-\zeta\omega t}}{\omega\sqrt{1-\zeta^2}} \sin \sqrt{1-\zeta^2}\omega t \quad (5)$$

Because damping is directly proportional to the viscosity of the fluid in the sample cell, substituting a liquid such as ethanol [$\eta(20°C) = 1.2$ cps] for water [$\eta(20°C) = 1.0$ cps] will increase the damping and, consequently, decrease the resultant vibrational displacements yielding the background noise. Therefore, it was believed that the substitution of an immersion medium with a 20% higher viscosity might improve the resolution of the AFM, and the resultant increase in resolution might permit the pore structure in the 10K polyethersulfone ultrafiltration membrane to be observed. It is the purpose of this paper to present and to discuss the results of such an examination with ethanol substituted for water as the immersion fluid.

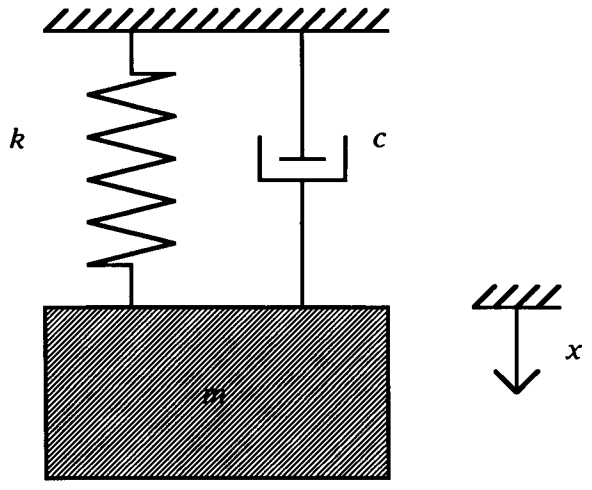

Figure 2 Model of AFM sensor in which m is the mass of the cantilever and tip, x is its displacement, k is the spring constant, and c is the damping constant.

EXPERIMENTAL

The 10K polyethersulfone ultrafiltration membrane selected for this study is commercially available from BIOKEN Separations. It is fabricated from a proprietary formulation that is cast on a nonwoven polyolefin fabric substrate and subsequently coagulated. This membrane has a sharp molecular weight cutoff (MWCO) and a high water flux rate. The performance of the membrane (pure water flux, water flux with dissolved protein, and percent protein rejections) is determined using 44 mm-diameter membrane disks in Amicon 8050 magnetically stirred ultrafiltration cells at room temperature and 55 psig. Each sample is tested in triplicate.

The proteins used to challenge the membrane were purchased from Sigma Chemical Co., St. Louis, MO. The concentrations of proteins in the permeate and retentate solutions were determined from their absorbences using a Perkin-Elmer Lambda 3A UV/visible spectrophotometer. The wavelengths at which the absorbences were measured are 360 nm for vitamin B-12 and 409 nm for myoglobin. Vitamin B-12 has a molecular weight of 1400 Daltons and myoglobin of 17,500 Daltons. The performance data

used to characterize the membranes were obtained using wet membranes, which had been stored in 18 Mohm-cm water in the refrigerator prior to testing.

The sample for evaluation by AFM was placed in a polyethylene bag with 18 Mohm-cm ultrapure water to maintain the moisture level. The polyethylene bag was then heat-sealed and subsequently shipped to Digital Instruments, Inc., of Santa Barbara, CA, for examination using the Nano-Scope AFM. Upon receipt, a small section (1×1 cm) was cut from the center of the membrane sheet for examination. This section was placed in ethanol for about 5 s and then exposed to air for 2–3 min to allow the excess ethanol on its surface to evaporate. It was then placed in the AFM sample cell and covered with ethanol. The sample was repeatedly scanned over a 2-h period. The AFM images used as figures in this paper were obtained after 2 h exposure to ethanol.

To determine the influence of ethanol exposure on the 10K polyethersulfone membrane pore structure, samples were immersed in ethanol for 2 h and subsequently tested immediately after rinsing in 18 Mohm-cm water or after 2 d exposure to 18 Mohm-cm water. These performance characteristics were also obtained by measuring the samples in triplicate.

RESULTS AND DISCUSSION

The initial scans of the surface of the 10K polyethersulfone ultrafiltration membrane yielded relatively smooth, monotonous images. These images are reminiscent of those obtained from the 10K polyethersulfone ultrafiltration membrane examined during water immersion and presented in an earlier paper in this series.[10] However, the AFM images improved with time so that fine detail could be detected after 30 min exposure to ethanol. The surface structure of the 10K polyethersulfone membrane immersed in ethanol as revealed by the AFM is shown in Figures 3–8. Figure 3 is a top-view image, i.e., the picture is perpendicular to the horizontal plane, of an area approximately 500×500 nm. The color bar at the right side of the image indicates the vertical deviation of the sample with the white regions being the highest points, and the dark regions, the depressions. Although it is not possible to determine *a priori* which dark regions are pores, numerous dark structures reminiscent of pores can be detected in this AFM image.

The AFM permits the measurement of distance variations in the sample's surface, as seen in Figures 4 and 5. An insert with a line traversing it can be seen in the lower left corner of each figure. These lines yield profiles of the surface structure and are shown in the upper portion of each figure. Distance variations along these profiles are determined by measurements of the horizontal and vertical distances between pairs of cursors, which are also shown. These measurements indicate that the pores are 7–9 nm in diameter, which is equivalent to the pore diameter expected for a 10,000 MWCO ultrafiltration membrane.[12] The size of the AFM tip limits its penetration into the pores, which appears to be less than 0.9 nm for these ultrafiltration membranes.

The sample can also be viewed at pitch angles other than perpendicular to the horizontal plane, as seen in Figures 6–8. Figures 6 and 7 were obtained using a 60° pitch angle and vary in their scan sizes. Figure 6 shows an area approximately 125×125 nm. Figure 8 was obtained at a 30° pitch angle with a scan size area of 900×900 nm. When the surface is examined at these pitch angles, the surface structures can be observed from a different perspective, and these features can be made more pronounced by expansion of the z-axis. The scale of the z-axis in Figure 6 is 10 times that used for the xy-plane. Consequently, structures that appear hemispherical in Figure 6 are in reality 10 times larger across their base in the xy-plane than in their heights as reflected by their z-axis image. Similarly, Figures 7 and 8 show fourfold and 15-fold expansions of their z-axis over xy-planes, respectively. Therefore, measurements of the surface features of Figure 8 indicate that the conical structures are around 45 nm at their bases and 2 nm in their heights. These structures result from portions of impinging assemblies of nodule aggregates that constitute the surface of the ultrafiltration membrane. Only a fraction of the volume of each assembly of nodule aggregates is revealed. The remainder is submerged within the membrane skin.

Although substitution of ethanol for water as the immersion liquid improves the resolution of the AFM images, the improvement with exposure time was unexpected. An immediate improvement in resolution had been predicted. However, the membrane was dipped in ethanol for only a few seconds prior to its mounting in the AFM. It is doubtful that all water entrained in the pores of the membrane could exchange with the ethanol in such a short time. Therefore, water and ethanol continue to exchange by diffusion after the sample placement in the instrument. Therefore, it is suspected that the gradual removal of water from the pores of the membranes and its replacement by ethanol caused the improvement of resolution with time.

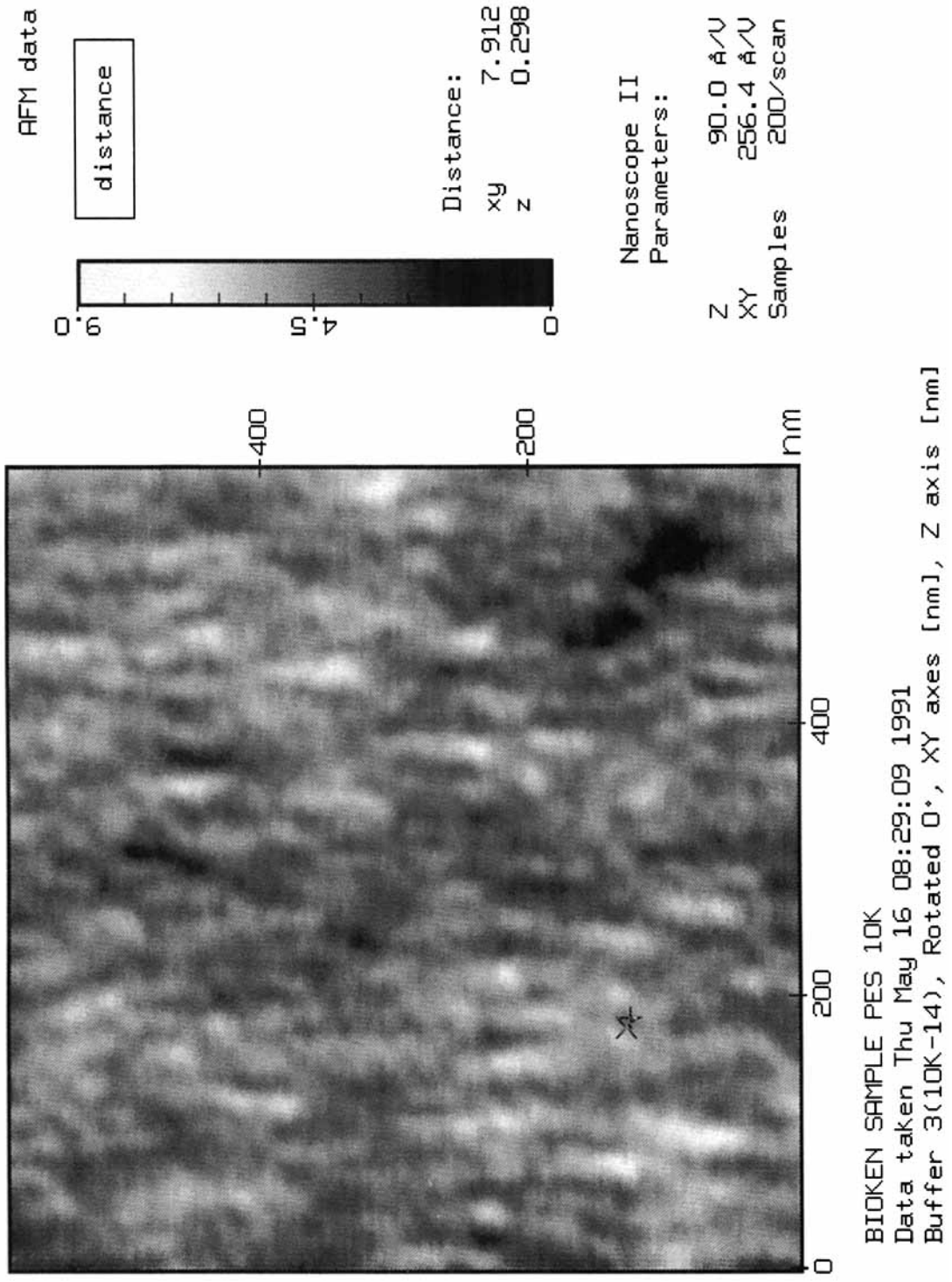

Figure 3 A top-view image of a 10K polyethersulfone ultrafiltration membrane surface taken with an AFM with color bar at right indicating the vertical deviation.

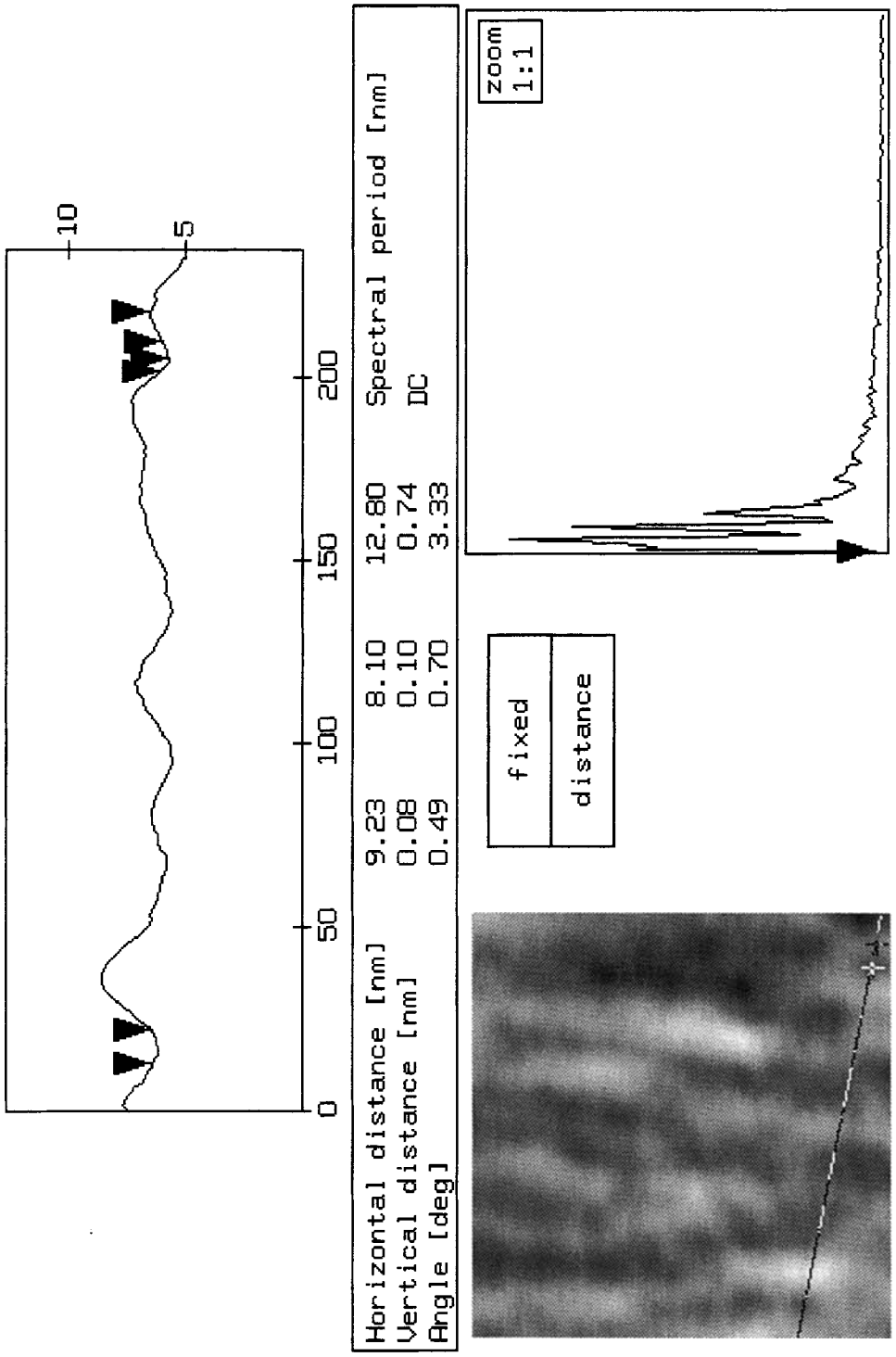

Figure 4 A vertical displacement profile of a 10K polyethersulfone ultrafiltration membrane surface taken from diagonal line across insert image by AFM.

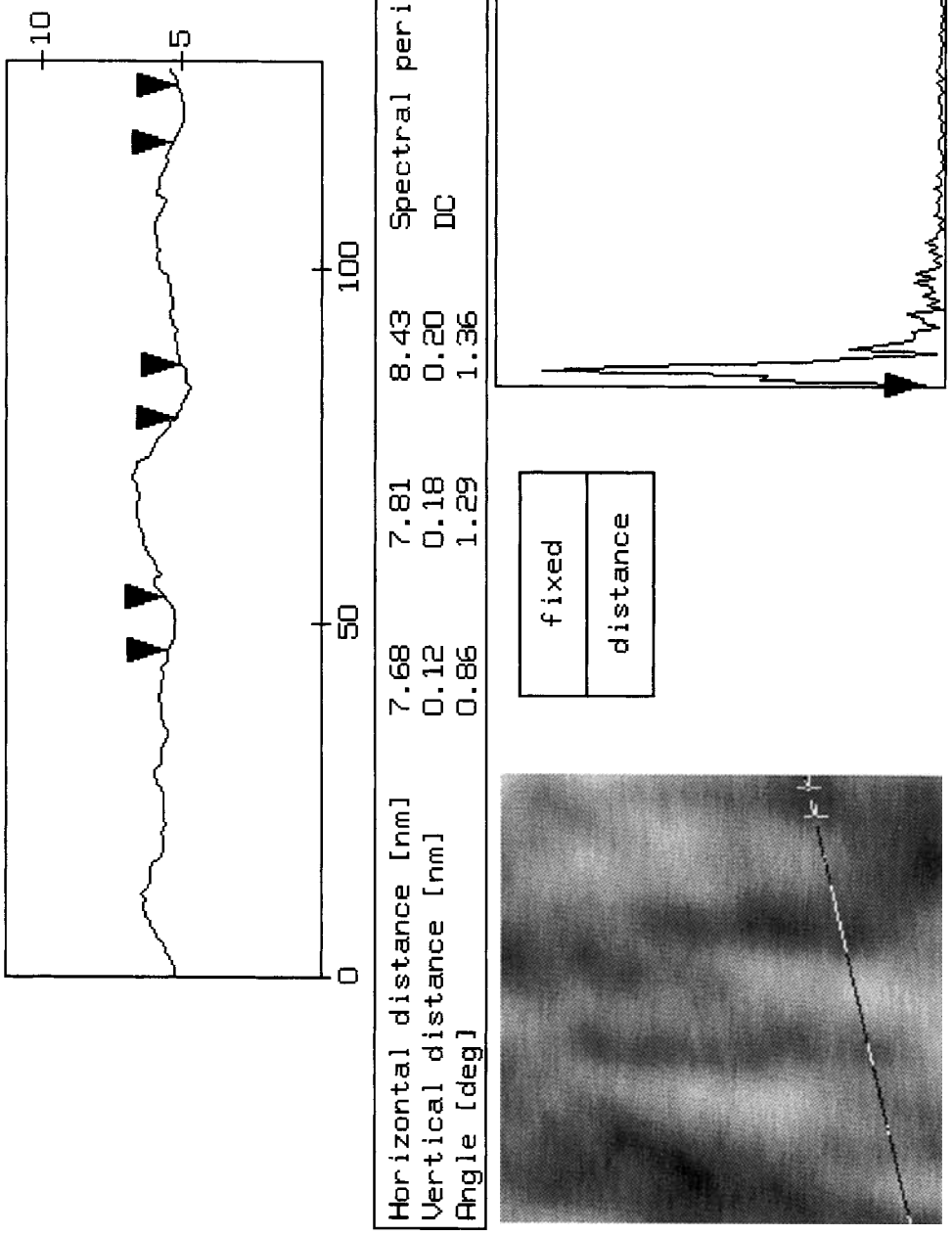

Figure 5 A vertical displacement profile of a 10K polyethersulfone ultrafiltration membrane surface taken from diagonal line across insert image by AFM with cursor pairs more readily identified.

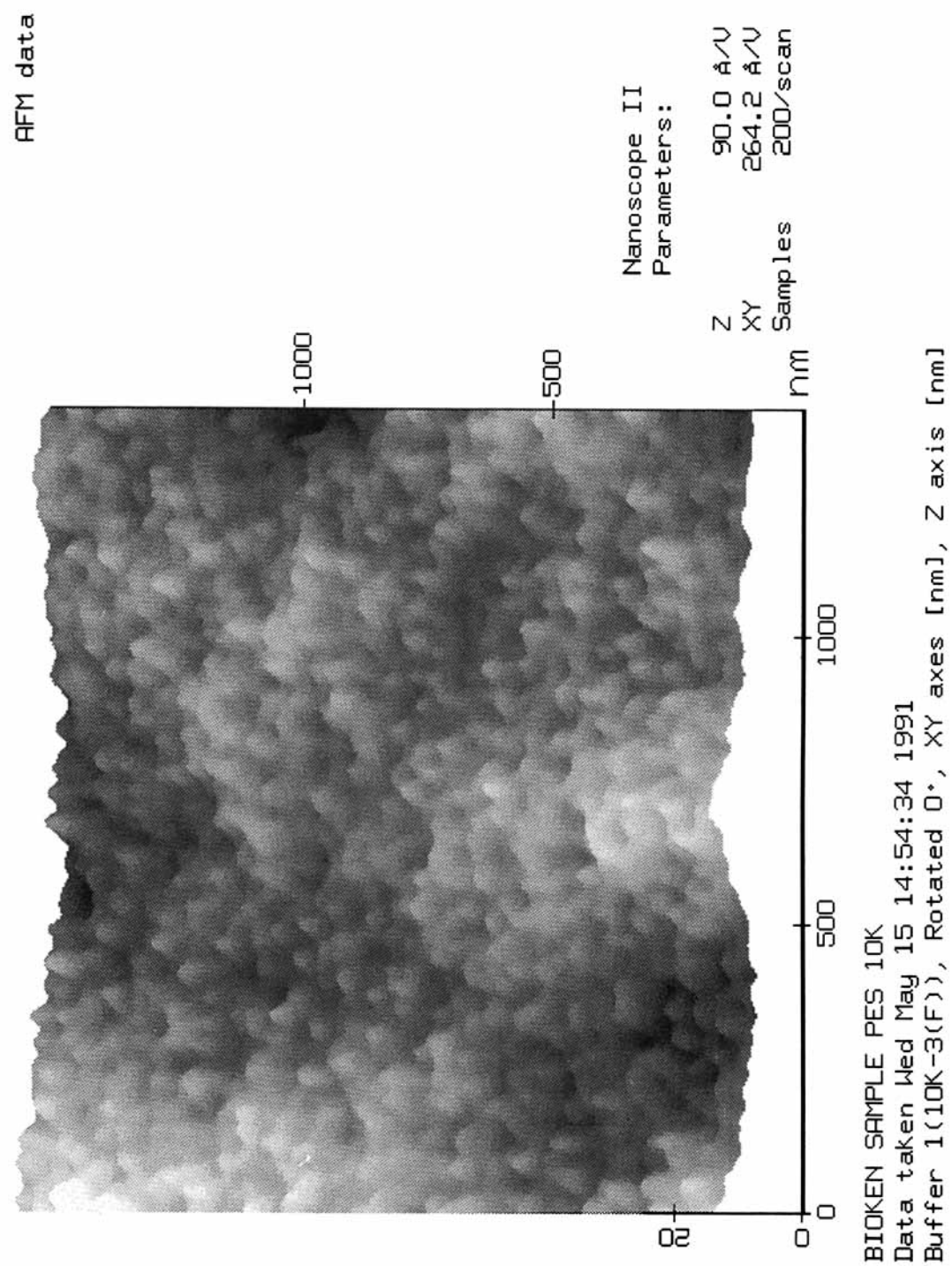

Figure 6 A 3D surface image of a 10K polyethersulfone ultrafiltration membrane at a 1500 × 1500 nm scan size and 60° pitch angle.

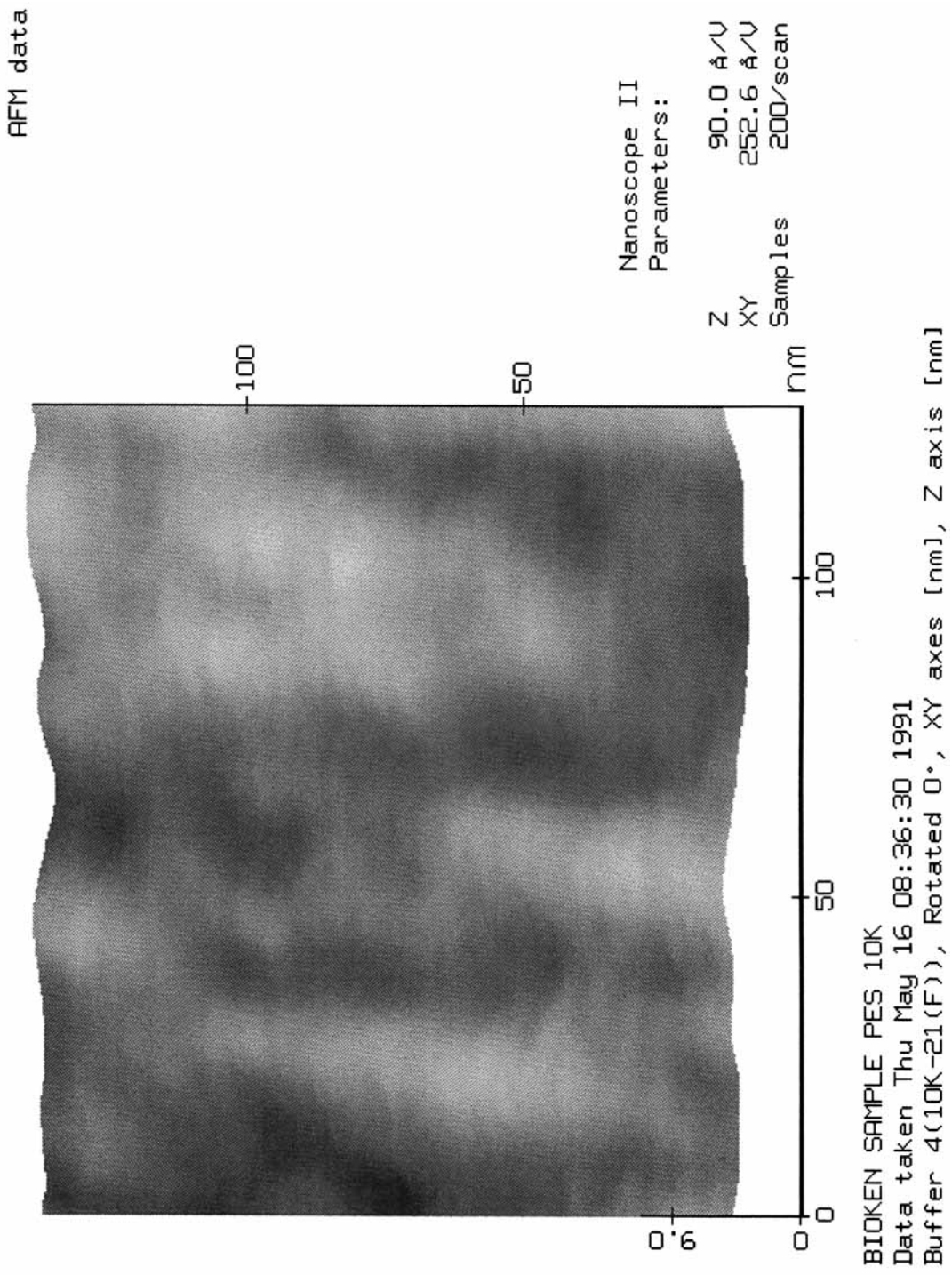

Figure 7 A 3D surface image of a 10K polyethersulfone ultrafiltration membrane at a 125 × 125 nm scan size and a 60° pitch angle.

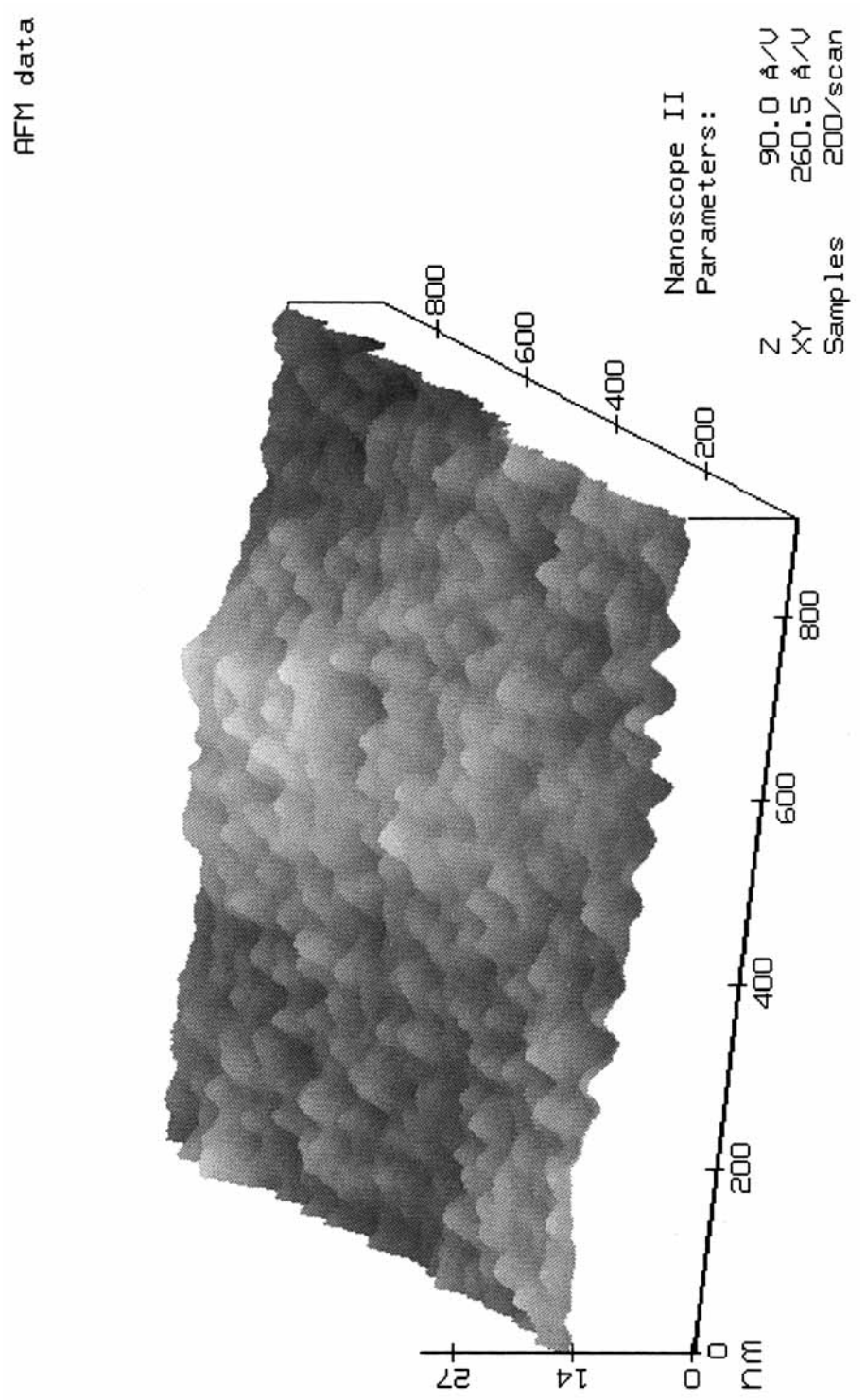

Figure 8 A 3D surface image of a 10K polyethersulfone ultrafiltration membrane at a 900 × 900 nm scan size and at a 30° pitch angle.

However, another possibility is that the ultrafiltration membrane swelled as it gradually absorbed ethanol into its polymer matrix. Swelling of the membrane simultaneously increases the diameter of its pores. The extent of such dimensional changes can be readily estimated by water flux measurements. The flow rate is directly proportional to the fourth power of the pore radius as described by the Poiseuille equation:

$$F = \frac{\pi p r^4}{8 l \eta} \tag{6}$$

where F is the flow rate; p, the pressure differential across the membrane; r, the pore radius; l, the pore length; and η, the fluid viscosity. Consequently,

$$\left(\frac{r_0}{r_t}\right) = \left(\frac{F_0}{F_t}\right)^{1/4} \tag{7}$$

where r_0 and r_t are the radii of the pores initially and after ethanol exposure, respectively, and F_0 and F_t are the corresponding flow rates.

Membranes were characterized after an ethanol dip for 5 s, after immersion in ethanol for 2.5 h, and after 2.5 h of ethanol immersion followed by 48 h immersion in water. The results are given in Table I. The increase in mean water flux from the control samples that were only dipped in ethanol to the samples that were immersed in ethanol for 2.5 h represents an increase in the pore radius of less than 6%. This increase is too small to account for the dramatic improvement in the resolution of the AFM images with time. However, the results do show that ethanol exposure does induce small, irreversible changes in the membrane.

Extended exposure to water (48 h) after ethanol exposure does not return the membrane's water flux or percent myoglobin rejection to their original values. These irreversible changes are a result of the nonequilibrium nature of the glassy state. Ethanol absorption facilitates configurational rearrangement of the polymer chains that also can alter the pore dimensions.

Ultrafiltration membranes separate molecules in solution on the basis of size, and they are classified according to molecular weight cutoff (MWCO) by membrane manufacturers. The molecular weight at which the membrane exhibits at least a 90% rejection of the challenge protein defines its MWCO. Yet, the reliance on MWCO to characterize membrane pore size is often misleading. Proteins adsorb onto the surfaces of membranes, altering both pore dimensions and performance. Protein adsorption is impacted by numerous factors including the relative hydrophobicity of the membrane, its surface charge, its rugosity, etc. Often, large discrepancies in the percent rejections of the protein by the membrane are seen if samples for analysis are taken from both the permeate and retentate portions of the challenge sample. Furthermore, variations in the measured percent rejection can be observed with the same protein if taken from different lots due to differences in their compositions, i.e., purity. Also, differences in the conformation of one protein to another in solution as well as their relative ability to adsorb on the membrane may yield misleading results.

Consequently, experimental techniques that yield direct measurements of membrane pore size are needed to classify ultrafiltration membranes, and scanning electron microscopy has been extensively applied for this purpose. However, not only do electron-beam instruments possess inherent limitations, but sample preparative techniques, such as freeze drying and solvent-exchange procedures to eliminate water, also alter the pore structure of many membranes. In contrast, the applications of AFM eliminate the need for often lengthy and tedious sample preparation techniques, which may also alter the pore structures of the ultrafiltration membranes. Liquids other than ethanol and water may be used

Table I Performance of Polyethersulfone Ultrafiltration Membranes after Ethanol Exposure

	Ethanol Dip (5 sec.)	Ethanol (2.5 h)	Ethanol and Water
Water flux (LMH)[a]	638 ± 124	800 ± 50	755 ± 63
Water flux with vitamin B-12 (LMH)	440 ± 44	556 ± 41	—
% Rejection vitamin B-12	8.6 ± 3.1	9.3 ± 0.8	—
Water flux with myoglobin (LMH)	127 ± 3.0	151 ± 12	146 ± 5
% Rejection myoglobin	99.0 ± 0.1	82.4 ± 1.1	85.8 ± 1.1

[a] LMH, liters per square meter per hour.

as immersion fluids, and the facility of operation of the AFM permits rapid screening of potential immersion liquids to identify those that are most compatible with any given membrane.

CONCLUSIONS

The atomic force microscope (AFM) is an effective tool with which to investigate the surface topography and measure the pore dimensions of ultrafiltration membranes. Samples can be examined by AFM without preparative procedures that can alter the membrane structure, such as the need for solvent exchange prior to high-vacuum coating in scanning electron microscopy. Furthermore, ultrafiltration membranes can be investigated while immersed in liquids, such as water and ethanol. It was shown that the resolution of the AFM image was improved with the substitution of ethanol for water as the immersion medium. It is believed that the improvement in resolution results from increased damping of the noise in the system due to the higher viscosity of ethanol than water. The resolution of the fine structure improved with ethanol exposure time. It is suspected that this enhancement results from the diffusion of entrained water from the membrane pores and its replacement with ethanol.

The authors wish to express their gratitude to Selly Sabach for typing this manuscript.

REFERENCES

1. G. Binnig, C. F. Quate, and Ch. Gerber, *Phys. Rev. Lett.*, **56,** 930 (1986).
2. P. K. Hansma, V. B. Elings, O. Marti, and C. E. Bracker, *Science,* **242,** 209 (1988).
3. G. Binning, Ch. Gerber, E. Stoll, T. R. Albrecht, and C. F. Quate, *Europhys. Lett.*, **3,** 1281 (1987).
4. T. R. Albrecht and C. F. Quate, *J. Appl. Phys.*, **62,** 2599 (1987).
5. M. Thompson and V. Elings, *Am. Lab.*, **23,** 36 (1991).
6. J. N. Israelachvili, *Intermolecular and Surface Forces with Applications to Colloidal and Biological Systems,* Academic Press, New York, 1985.
7. D. Rugar and P. Hansma, *Phys. Today,* **40,** 23 (1990).
8. O. Marti, B. Drake, and P. K. Hansma, *Appl. Phys. Lett.*, **51,** 484 (1987).
9. B. Drake, C. B. Prater, A. L. Weisenhorn, S. A. C. Gould, T. R. Albrecht, C. F. Quate, D. S. Cannell, H. G. Hansma, and P. K. Hansma, *Science,* **243,** 1586 (1989).
10. A. K. Fritzsche, A. R. Arevalo, A. F. Connally, M. D. Moore, V. Elings, and C. M. Wu, *J. Appl. Polym. Sci.,* to appear.
11. R. K. Vierck, *Vibration Analysis,* 2nd ed. Harper and Row, New York, 1979.
12. The Filtration Spectrum, Osmonics, Inc., FS-8409 P/N17978.

Received July 9, 1991
Accepted October 24, 1991